communications earth & environment

Article

A Nature Portfolio journal

https://doi.org/10.1038/s43247-025-02152-0

Mixed-layer lipidomes suggest offshore transport of energy-rich and essential lipids by cyclonic eddies

Kevin W. Becker [1] ✉, Quentin Devresse [1,3], Xavier Prieto-Mollar[2], Kai-Uwe Hinrichs[2] & Anja Engel [1]

Mesoscale eddies are ubiquitous features in the ocean affecting the cycles of nutrients and carbon. Cyclonic eddies formed in Eastern Boundary Upwelling Systems can substantially modulate primary production by phytoplankton and the vertical and lateral export of organic carbon. However, the impact of eddy activity on the biochemical composition of eukaryotic phytoplankton, bacteria and archaea and associated consequences for carbon and energy flows are largely unknown. Here, we investigated the microbial lipidome in the surface ocean in and around a cyclonic eddy formed in the coastal upwelling system off Mauritania. We show that the eddy contained almost three times the amount of lipids compared to the surrounding open-ocean and coastal waters. The eddy lipid signature with energy-rich triacylglycerols and essential fatty acid-containing membrane lipids of eukaryotic phytoplankton origin was further significantly different from the ambient waters. Strong variability in lipid distributions within the eddy was related to differences in microbial community composition. Estimates indicate that in the Mauritanian upwelling area, as much as 9.7 ± 2.0 gigagrams of lipid carbon per year is delivered to the open ocean by coastal cyclonic eddies potentially fueling higher trophic levels and contributing to the maintenance of secondary productivity and carbon export offshore.

Marine microbes are key players in global biogeochemical cycles including the carbon and nutrient cycles. About half of the global primary production occurs in the surface ocean via photosynthesis by phytoplankton[1], which provides the basis for the transfer of organic matter and energy to marine ecosystems, supporting most marine food webs including fisheries production, and plays a critical role in ocean carbon sequestration[2]. Changes in the marine environment resulting from physical and chemical processes impact phytoplankton growth by providing access to light and nutrients. For example, upwelling of nutrient-rich subsurface water sustains high productivity in the ocean's eastern boundary currents, while in the surface waters of the open-ocean subtropical gyres, productivity is limited by the supply of nutrients[3]. Besides these large-scale oceanographic features driving productivity patterns in the global ocean, smaller scale processes affecting areas of about 10–100 km, i.e. mesoscale processes, are important for shaping anomalies in productivity. One of the most prominent mesoscale features in the ocean are eddies, which are ubiquitous swirling currents that dominate local biogeochemical processes[4]. Eddies modulate light and nutrient conditions in the surface affecting abundance and activity of both phytoplankton and heterotrophic microbial communities[5–8]. Three types of eddies have been described: Cyclonic, anticyclonic and anticyclonic mode water eddies[9]. The three types show substantially different effects on community structure and food-web dynamics, with cyclones representing productive oases for marine life. By shoaling the pycnocline, cyclonic eddies can be sites of enhanced nutrient supply[10,11] and light availability[12] stimulating phytoplankton production. The stimulated phytoplankton activity has further been shown to attract zooplankton[13] and enhance carbon export fluxes[14,15]. In all of the eastern boundary upwelling systems (EBUS), mesoscale eddies are frequently observed[16,17]. Besides affecting biogeochemical cycling of carbon and nutrients locally, eddies formed in EBUS might contribute to the redistribution of nutrients and carbon from the coast to the open oligotrophic ocean due to their westward propagation[17–20]. Based on satellite-derived measurements of particulate organic carbon (POC) in the California current system, trapping and transporting coastal water offshore by mesoscale eddies has been estimated to result in a significant offshore POC enrichment[17]. The connectivity between coastal upwelling and open-ocean regimes may thus contribute to sustaining the

[1]GEOMAR Helmholtz Centre for Ocean Research Kiel, Kiel, Germany. [2]MARUM – Center for Marine Environmental Sciences and Faculty of Geosciences, University of Bremen, Bremen, Germany. [3]Present address: Department of Biological Oceanography, Leibniz Institute for Baltic Sea Research Warnemünde, Rostock, Germany. ✉e-mail: kbecker@geomar.de

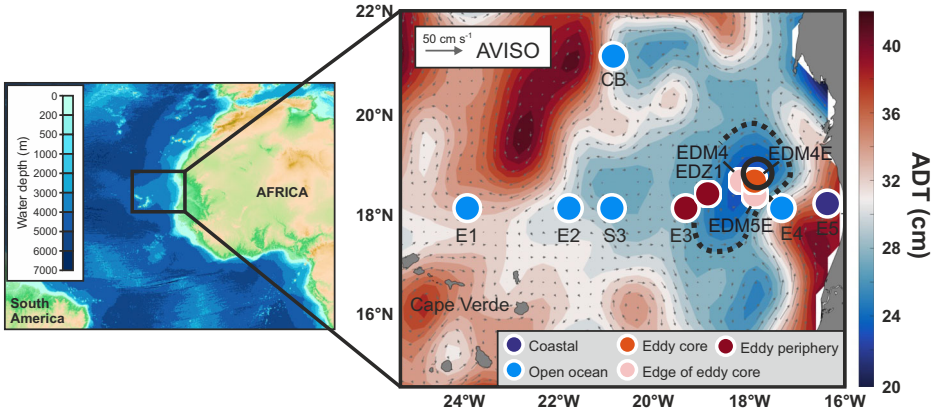

Fig. 1 | Sampling sites. Stations for lipidomics analysis collected during RV Meteor cruise M156 in the Eastern Tropical North Atlantic upwelling system off Mauritania. The gridded bathymetry map was obtained from http://www.gebco.net (General Bathymetric Chart of the Oceans, GEBCO 2024 Grid). The background in the zoom in shows the absolute dynamic topography (ADT) at the time of sampling obtained from https://www.aviso.altimetry.fr, last access: 23 July 2024, with the direction and speed of surface water geostrophic currents shown as arrows. Black circle indicates the eddy core and the dashed line indicates potential edge of the eddy-influenced area (eddy periphery). Colors of sampling stations indicate position with red colors representing eddy stations (red: eddy core, light red: edge of eddy core, dark red: eddy periphery) and blue colors outside stations (dark blue: coastal station, light blue: open-ocean stations). Station E3 appeared to be located just beyond the eddy periphery, but was shown to be within the eddy influenced area[7] and thus assigned to be within the eddy periphery. While station E4 was located within the coastal-boundary current region, our lipid analysis revealed a high similarity to the open-ocean stations rather than the coastal station E5 and was assigned as open-ocean station.

biological productivity in the oligotrophic ocean, which has been a long-standing conundrum[21–23].

To date, biogeochemical studies of mesoscale eddies have focused primarily on bulk measurements of, for example, POC and dissolved organic carbon or primary production, while the effects of mesoscale eddies on changes in the biochemical composition of organic matter as well as the biogeochemical consequences of these for the ocean's carbon cycle remain poorly constrained. One important component of the oceanic organic matter composition are microbial lipids[24], which can make up to 20% of the surface ocean particulate organic matter pool[25] and are produced and used by organisms from all three domains of life for energy storage, membrane structure, signaling and electron transport. Lipid biomarkers have mainly been used to study specific biological and chemical processes in the ocean, such as nutrient limitation[26], but recent advances in lipidomics analysis using high resolution mass spectrometry[27] enable the detection of hundreds to thousands of individual lipids in environmental samples. For example, a recent study by Holm et al.[28] provided evidence for global-scale lipidome remodeling in surface ocean phytoplankton as a function of temperature. Lipids also carry coarse chemotaxonomic information that allows to distinguish the dominant microbial groups in the marine water column, such as different phytoplankton, heterotrophic bacteria, and archaea[29–31]. The observed effects of eddies on the distribution of microbes[5,6] can thus be expected to be reflected in variations in the lipidome. Additionally, the lipidome of phytoplankton is one of the primary determinants of their nutritional quality[32] and alterations in the types and amounts of lipids produced due to changes induced by mesoscale eddies will affect the activity and population dynamics of organisms at higher trophic levels and ultimately carbon export from the surface to the deep ocean.

Here, we investigated the surface microbial lipidome in and around a cyclonic eddy formed in the highly productive Mauritania EBUS in the Eastern Tropical North Atlantic (Fig. 1, see Supplementary Methods including Supplementary Figs. 1–3 for detailed eddy identification) where mesoscale eddies commonly occur[16,33]. Surface mixed-layer samples, where lipid abundances are typically highest[25,30,34], were taken within the core, the edge of the core, and the periphery of the eddy. Samples outside the eddy were collected along a 18°N transect between the Cape Verde islands and the coast where the samples to the West of the eddy represent open-ocean sites. In previous studies, we showed that bulk microbial metabolic activities and abundances, and bulk pools of organic matter (POC and dissolved organic carbon) were significantly enhanced in the eddy studied with strong horizontal variability within the surface of the eddy[7,35,36]; this variability was covered by our sampling scheme for lipid analysis. The stimulated microbial growth in this cyclone might provide fresh organic matter to the open ocean during westward propagation. We sought to further elucidate microbial carbon cycling in this system through the lens of lipidomics and to examine the factors that determine ocean lipid composition at the mesoscale. Since mesoscale eddy activity is predicted to change as a result of climate change[37], it is crucial to know how these features affect the lipid composition in order to better assess consequences for food web dynamics and carbon export.

Results and discussion

Lipidome variations in and around a cyclonic eddy formed in the EBUS off Mauritania

In total, almost 900 individual lipid species were identified in the mixed layer in and around the cyclonic eddy sampled during the RV Meteor cruise M156 (see Supplementary Table 1 for mixed-layer depths). Hierarchical clustering analysis using Euclidian distances of the lipidome (see Supplementary Figs. 4–6 for chemical structures and mass spectral identification) from all mixed-layer samples showed two main clusters of samples (Fig. 2). The first cluster contains the samples from all open-ocean stations and the coastal stations, while the second cluster only contained samples from inside the eddy as well as station E3, which was just beyond the eddy periphery and has been shown to be influenced by the cyclonic eddy in our earlier work[7]. The stations outside of the eddy further clustered into two subclusters: coastal and open-ocean stations. While station E4 was located within the coastal-boundary current region, it clustered together with the open-ocean stations rather than the coastal station E5. Within the eddy-influenced area, there are three subclusters: samples from the core of the eddy, the edge of the core, and the periphery. Thus, the eddy carries a distinct mixed-layer lipid signature with variability depending on the position within the eddy-influenced area.

Sources of lipid groups in the identified clusters

Our lipidome analysis covered lipids from four main categories: 1. intact polar lipids (IPLs), which are structural membrane components, 2. respiratory quinones, which are lipid-soluble electron and proton carriers, 3. pigments, which are involved in photosynthesis, and 4. triacylglycerols (TAGs), which are energy storage molecules. Most of these lipid groups showed significant differences in concentration between the eddy-influenced stations and stations outside of the eddy (one-way ANOVA,

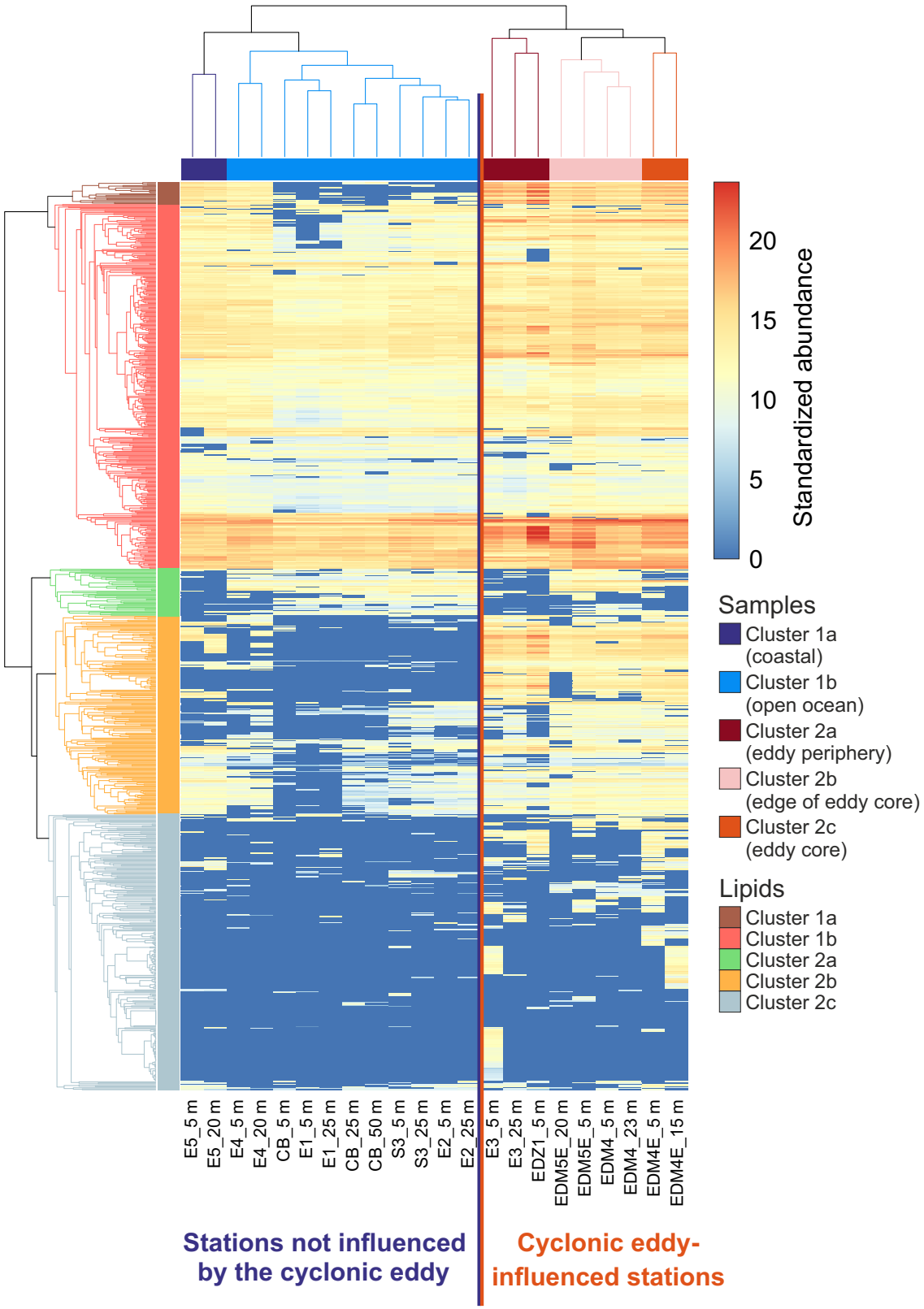

Fig. 2 | Heatmap visualization of lipid concentrations and hierarchical clustering. Heatmap of log-transformed lipid concentrations (893 individual lipids) in mixed-layer samples collected during M156 in and around a cyclonic eddy formed in the upwelling system off Mauritania (see Supplementary Table 1 for mixed-layer depth of each station). Hierarchical clustering analysis of columns (samples) and rows (lipids) was performed using Euclidean distances. The samples clustered according to their relative location within the cyclonic eddy and the ambient waters. The locations of the stations are shown in Fig. 1. Each of the lipid (sub)clusters contained an array of molecularly diverse lipids from the four main categories: 1. intact polar lipids, 2. respiratory quinones, 3. pigments, and 4. triacylglycerols as described in main text. The cluster analysis with fully annotated lipids is provided in Supplementary Fig. 14.

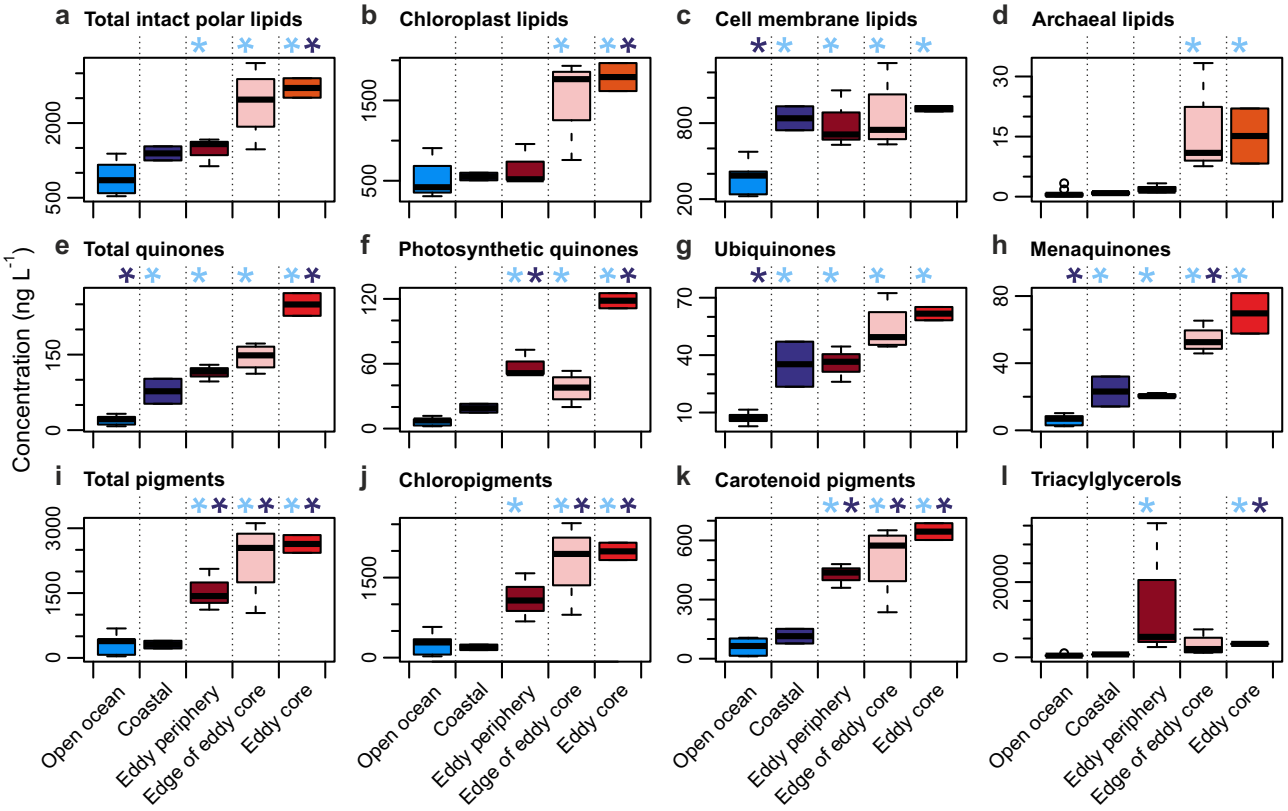

Fig. 3 | Lipid group concentrations in the identified clusters. Average concentration of total intact polar lipids (**a**), chloroplast lipids (**b**), cell membrane lipids (**c**), archaeal lipids (**d**), total quinones (**e**), photosynthetic quinones (**f**), ubiquinones (**g**), menaquinones (**h**), total pigments (**i**), chloropigments (**j**), carotenoid pigments (**k**), and triacylglycerols (**l**) in the five sub-clusters of sampling stations identified by the hierarchical clustering analysis of surface mixed-layer samples collected during M156 off Mauritania. Boxes represent the interquartile ranges, the line within the box the median, and the whiskers extend to the minimum and maximum values within 1.5 times the interquartile range. Outliers are shown as circles. Asterisks indicate variables significantly different (one-way ANOVA, $p < 0.05$) from coastal (dark blue) and open-ocean (light blue) stations, respectively. The chloroplast lipids are the sum of glycolipids with diacylglycerol side chain, including the galactolipids mono- and digalactosyldiacylglycerol and the sulfolipid sulfoquinovosyldiacylglycerol. The cell membrane lipids include all phospho- and betaine lipids. The archaeal lipids contain all core and intact polar diether and tetraether lipids. The respiratory quinones are separated into photosynthetic quinones (plastoquinone and vitamin K1), ubiquinones and menaquinones. The pigments are divided into chloropigments, which is the sum of chlorophylls and related compounds (porphyrin ring-containing molecules) and carotenoid pigments, which include all xanthophylls (e.g., fucoxanthin and zeaxanthin) and β-carotene. For an overview of the chemical structures, the reader is referred to Supplementary Fig. 4.

$p < 0.05$, Fig. 3). IPLs, quinones and pigments were most abundant in the eddy-influenced stations with the highest concentrations in the core and at the edge of the core. For example, concentrations of IPLs in the core of the eddy were found to be on average three times higher than in the open ocean, and pigment concentrations were even nine times higher, indicating enrichments in microbial and in particular photosynthetic biomass (Fig. 3a). TAGs were also more abundant in the eddy, but showed particularly high concentrations in samples from the eddy periphery (Fig. 3l). Here, TAGs were by far the most abundant lipid group in the eddy-influenced stations where total lipids contributed more than 6% to the POC pool in the eddy periphery, whereas the contribution was only ~2% for the coastal open-ocean stations (Supplementary Fig. 7). The large spread in TAG concentrations in the periphery is due to the extremely high concentrations in the sample from station EDZ1, which showed six times higher concentrations than the sample from the same depth from the other station in the eddy periphery (station E3, Supplementary Data File). TAGs are used by mainly by eukaryotic phytoplankton as energy reserves and TAG accumulation often occurs in growth limiting conditions such as dissolved inorganic nutrient (nitrogen) deprivations[38]. However, nutrient limitation was not observed in the periphery of the sampled cyclonic eddy as we could show based on dissolved inorganic nutrient profiles in our previous study[7]. Responses to the daily light cycle can also influence the TAG content in phytoplankton[39] and some of the observed variability in TAG concentration may be related to the time of sampling; station EDZ-1 was sampled at the end of the day when TAG concentrations are highest, while station E3 was sampled at the end of the night when TAG concentrations are lowest (see Supplementary Table 1 for sampling information). However, all other stations within the eddy were also sampled at the end of the night or the early morning when daily TAG concentrations in phytoplankton are low[39]. We thus attribute the high TAG concentrations in the periphery of the eddy mainly to eukaryotic phytoplankton biomass that is particularly rich in TAGs. This is in line with our previous observation of the presence of large (>20 µm) eukaryotic phytoplankton in the periphery of this eddy based on combined chlorophyll *a* (Chl *a*) measurements, ^{14}C-based primary production rates and flow cytometry analyses[7].

The main lipid groups were further broken down into groups according to their sources and/or function. This revealed that the higher IPL concentrations in the eddy are mainly due to higher concentrations of chloroplast membrane lipids, i.e., the galactolipids monogalactosyl- (MGDG) and digalactosydiacylglycerol and the sulfolipid sulfoquinovosyldiacylglycerol (see Fig. 3b), which are of phytoplankton origin including both eukaryotic phytoplankton and cyanobacteria[30]. Similarly, within the pigments, we observed significantly higher concentrations of chloropigments and carotenoid pigments in the eddy-influenced stations compared to stations outside of the eddy (Fig. 3j, k), which are used by phytoplankton to perform photosynthesis. In contrast, cell membrane lipids, which include all phospholipids as well as betaine lipids (see Supplementary Fig. 4 for chemical structures), were only significantly higher in concentration in the eddy compared to the open ocean, but similar compared to the coastal samples (Fig. 3c). These lipids primarily originate from eukaryotic

phytoplankton and to some extent of heterotrophic bacteria in surface ocean samples[30]. The higher concentration of chloroplast lipids together with the invariant concentration of cell membrane lipids in the eddy compared to the coastal station suggests higher abundances of cyanobacterial cells relative to eukaryotic phytoplankton in the core region of the cyclonic eddy, which is in line with our previous flow cytometry analysis[7]. This is further supported by the significantly higher concentration of photosynthetic quinones [plastoquinone and vitamin K1] in the core of the eddy compared to the other stations and the invariant ubiquinone (UQ) concentration (Fig. 3f, g) between those regions. While in eukaryotic algae UQ and photosynthetic quinones function as electron transporters in the electron transport chain of oxygenic photosynthesis and the aerobic respiratory chain, respectively, cyanobacteria only contain photosynthetic quinones and use plastoquinone in the electron transport pathways of both photosynthesis and respiration[40]. Higher abundances of cyanobacteria in the core of the eddy also explain the relatively low TAG, but high IPL and pigment concentrations in this part of the eddy, because naturally occurring cyanobacteria are not known to accumulate notable amounts of TAGs[38]. In several cultures of oceanic cyanobacteria that dominate in the study area, such as *Synechococcus* and *Prochlorococcus*[41], even no TAGs were detected[39], consistent with the lack of TAG biosynthesis in these groups[42].

We additionally observed menaquinones (MKs) to have a similar concentration range as the photosynthetic quinones and UQs (Fig. 3h) and, similar to the photosynthetic quinones, MKs were significantly more abundant in the core region of the eddy compared to the coastal and open-ocean stations. The detected MKs were all fully unsaturated, i.e., they contained one double bond per isoprenoid unit and are thus of bacterial origin[40]. Typically, bacterial MKs are involved in anaerobic metabolism due to their low redox potential, while they cannot operate efficiently under aerobic conditions[40]. Accordingly, in the marine water column, bacterial MKs have so far only been found in the anoxic waters of the Black Sea[43]. In gram positive bacteria, however, MK biosynthesis, which is evolutionary the most ancient pathway of quinone biosynthesis[44], is conserved[45]. Gram positive bacteria, in particular Actinobacteria, have been shown to be abundant in the Mauritania upwelling region[41] making them a likely source of MKs that are particularly abundant in the core of the eddy.

Archaeal lipid concentrations were comparatively low, but showed highest values in the core and at the edge of the core of the eddy (Fig. 3d). The majority of the detected lipids were glycerol dibiphytanyl glycerol tetraethers (GDGTs) including intact polar and core crenarchaeol derivatives (see Supplementary Data File for all identified lipids), which are primarily derived from Nitrososphaerota (syn. Thaumarchaeota) in the marine water column[46]. For one station from the edge of the eddy core (station EDM5E), we obtained a depth profile down to 800 m, which showed that archaeal lipids had highest concentrations near the surface (20 m) within the surface mixed layer (Supplementary Fig. 8). This indicates that archaeal biomass is relatively enriched in the surface mixed layer at this station. Since the detected archaeal lipids mainly included core lipids and the intact polar lipids monohexose GDGTs (see Supplementary Data File), the differentiation between living and non-living archaeal biomass is difficult. It has been shown that archaeal IPLs, unlike bacterial and eukaryotic IPLs, may persist rapid degradation[47–49]. However, we have filtered only small volumes (1 L) of seawater and other archaeal IPLs might have simply been below the limit of detection. The dominance of monohexose GDGTs has further been observed in the marine water column from other regions and Nitrososphaerota were always suggested to be their dominant source[29,31]. Together with the distinct peak in concentration this points at least in part to the in-situ production of archaeal lipids in the surface mixed layer in and around the core of the cyclonic eddy. This was surprising to us, because Nitrososphaerota and their lipids are typically found to peak deeper in the water column[50,51]. The uplift of isopycnals in the cyclonic eddy brought nutrients including ammonia, which is the main substrate for Nitrososphaerota for energy generation[52], into the mixed layer of the core of the eddy[7] (Supplementary Fig. 9) and might explain their relatively high abundance at the shallow depth in our samples[53].

Mixed-layer-integrated concentrations of specific lipid biomarkers

The distribution of individual biomarker lipids integrated over the surface mixed layer provided further insights into the distribution of microbes within the eddy-influenced area and manifests the observations from the lipid group concentrations. The distribution of Chl *a* (Fig. 4a), a generic biomarker for oxygenic photosynthetic organisms, clearly showed enhanced values in the eddy-influenced stations, but different groups of the phytoplankton community contributed differently to the Chl *a* signal in the different regions within the eddy as indicated by specific biomarkers. Long-chain, polyunsaturated chloroplast (MGDG 38:6, a monogalactosyldiacylglycerol with 38 acyl carbons and six acyl double bonds) and cell membrane (PC 38:8, a phosphocholine diacylglycerol with 38 acyl carbons and eight acyl double bonds) as well as energy storage (TAG 54:10, a triacylglycerol with 54 acyl carbon and ten acyl double bonds) lipid biomarkers, all indicative of eukaryotic phytoplankton such as diatoms and dinoflagellates[54], were all particularly abundant in the stations from the periphery of the eddy (Fig. 4b–d). The high concentration of the carotenoid pigment fucoxanthin (Supplementary Fig. 7f) indicates that diatoms were the dominant eukaryotic phytoplankton group in this area of the eddy, which is in line with earlier studies[55,56]. In contrast, IPLs and pigments diagnostic for cyanobacteria, such as MGDG 30:1[30] and zeaxanthin[57], were elevated in the core and at the edge of the core of the eddy (Fig. 4e, f). As expected, divinyl Chl *a*, a unique biomarker for the cyanobacterium *Prochlorococcus*[58], occurred mainly in the open-ocean stations (Fig. 4g), consistent with their predominance in (sub)tropical oligotrophic waters[59]. This suggests that other cyanobacteria, e.g., *Synechococcus*, likely dominated the photosynthetic biomass in the core of the eddy, which is consistent with our previous flow cytometry analysis[7] and which has also been shown for other cyclonic eddies[60]. Similarly to the cyanobacterial lipids in the core, a short-chain, monounsaturated phosphatidylethanolamine with 30 acyl carbons (PE 30:1), which is derived primarily from heterotrophic bacteria in marine samples[30], was dominant in the surface mixed layer of the core of the eddy (Fig. 4h). The increased concentrations of $MK_{7:7}$ (Fig. 4i), which is likely derived mainly from gram positive bacteria[45] that may be involved in the degradation of complex polymers[61], is another indicator for abundant heterotrophic bacterial biomass and matches heterotrophic bacterial cell abundances quantified by flow cytometry from our previous study of this eddy[7]. The mixed-layer-integrated concentration of monohexose crenarchaeol (Fig. 4j), a diagnostic biomarker for ammonia oxidizing Nitrososphaerota[62], confirms their predominance in the core of the eddy core as outlined above. An example of a biomarker for the open-ocean stations is 19'Hexanoyloxy-4-ketofucoxanthin (Fig. 4k), which is indicative of haptophytes, in particular cocclithophores[63]. This is consistent with the general observation of increasing coccolithophore abundance from coastal to open-ocean regimes[64].

Variations in acyl side chain structure of the microbial lipids

We were interested in the detailed structure of the side chains of the acyl containing lipids, i.e., chloroplast lipids, cell membrane lipids and triacylglycerols, across the identified clusters. On the one hand this provides additional structural information and on the other hand unsaturated fatty acids, which make up the acyl chains, have nutritional properties important for higher trophic levels[54]. For example, phytoplankton are the main producer of essential fatty acids, such as eicosapentaenoic acid, in the marine environment. Essential fatty acids are important nutrients that higher trophic levels, such as zooplankton, cannot synthesize and must obtain from their diet[65]. Since our mass spectrometry analysis only allows glycerolipid identification to the lipid species level for some lipid groups (i.e., sum of carbon atoms and sum of double bonds on all fatty acyl moieties due to the lack of diagnostic MS/MS fragment ions, see Supplementary Figs. 5 and 6), the average number of total acyl carbon and total acyl double bonds (unsaturations) were calculated for each lipid group. We observed significant differences for both the number of acyl carbons and the degree of unsaturation for the chloroplast lipids in the periphery of the eddy

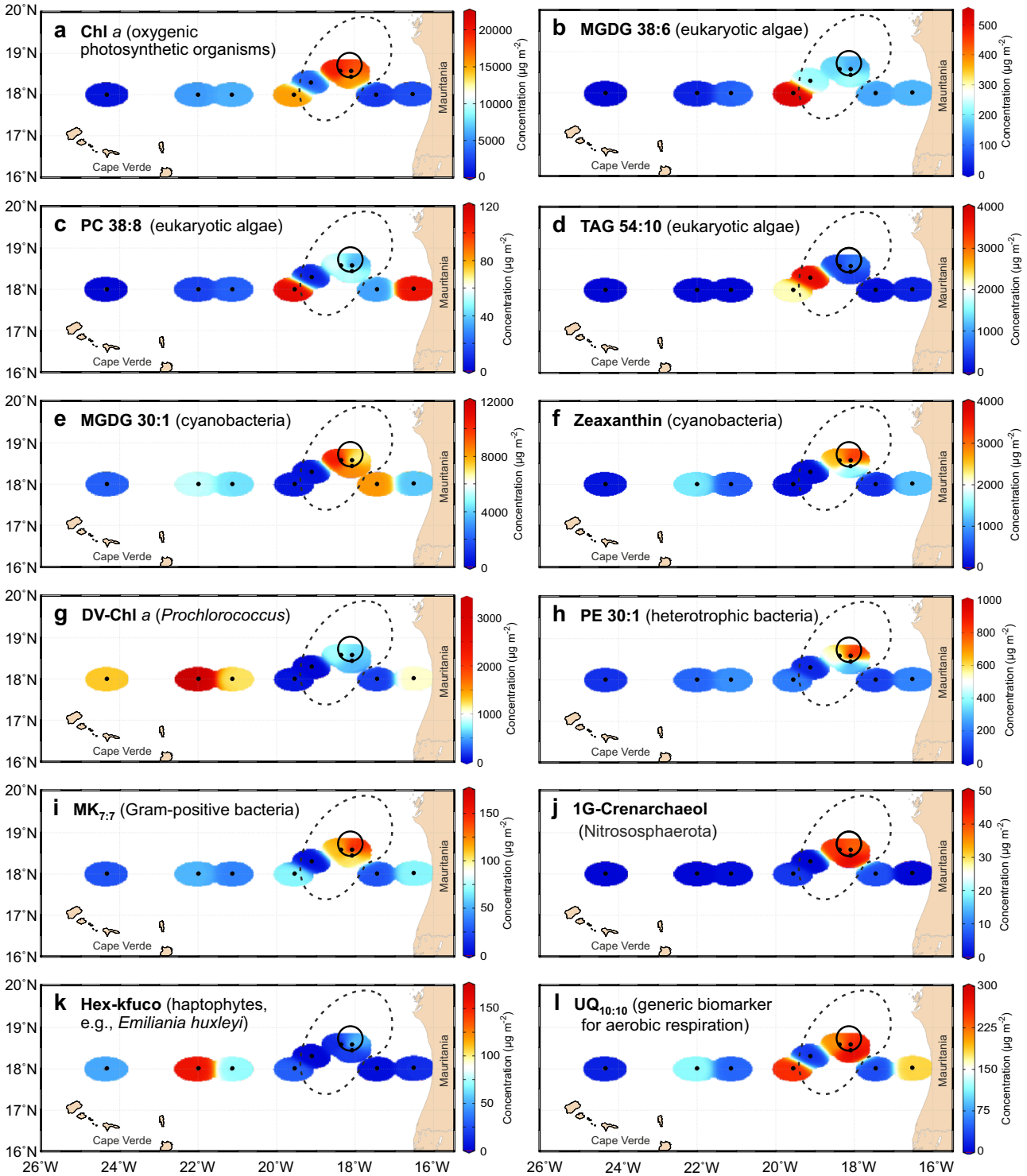

Fig. 4 | Mixed-layer-integrated concentrations of selected biomarker lipids. Concentrations of individual lipids representative of different microbial groups integrated over the surface mixed layer in samples collected in and around a cyclonic eddy off Mauritania. **a** chlorophyll *a* (Chl *a*) as biomarker for oxygenic photosynthetic organisms, **b**–**d** polyunsaturated fatty acid-containing intact polar and energy storage lipids indicative of eukaryotic algae, **e**, **f** a monounsaturated glycolipid (MGDG) and the carotenoid pigment zeaxanthin indicative of cyanobacteria, **g** divinyl (DV) Chl *a* diagnostic for *Prochlorococcus*, **h** a monounsaturated phospholipid (PG) indicative of heterotrophic bacteria, **i** a menaquinone (MK) indicative of gram-positive bacteria, **j** an intact Crenarchaeol diagnostic for Nitrososphaerota, **k** a carotenoid pigment (Hex-kfuco) indicative of haptophytes, and **l** a ubiquinone (UQ) as generic biomarker for aerobic respiration. The black circle indicates the eddy core and dashed line indicates potential edge of the eddy-influenced area (eddy periphery). For interpolation between data points, weighted-average gridding was used, which is integrated in Ocean Data View[103]. MGDG monogalactosyldiacylglycerol, PC phosphatidylcholine, PE phosphatidylethanolamine, TAG triacylglycerol, 1G monohexose, Hex-kfuco 19'Hexanoyloxy-4-ketofucoxanthin. Nomenclature of lipids: For intact polar diacylglycerol lipids and triacylglycerols the sum composition of acyl double bonds and acyl carbon atoms in each compound is provided as C a:b, where C indicates the lipid group, a the number of acyl carbons and b the number of acyl double bonds. For respiratory quinones, the nomenclature after Elling et al.[104] is used ($Q_{m:n}$) where Q indicates head group type, m the number of isoprenoid units in the side chain and n the number of double bonds.

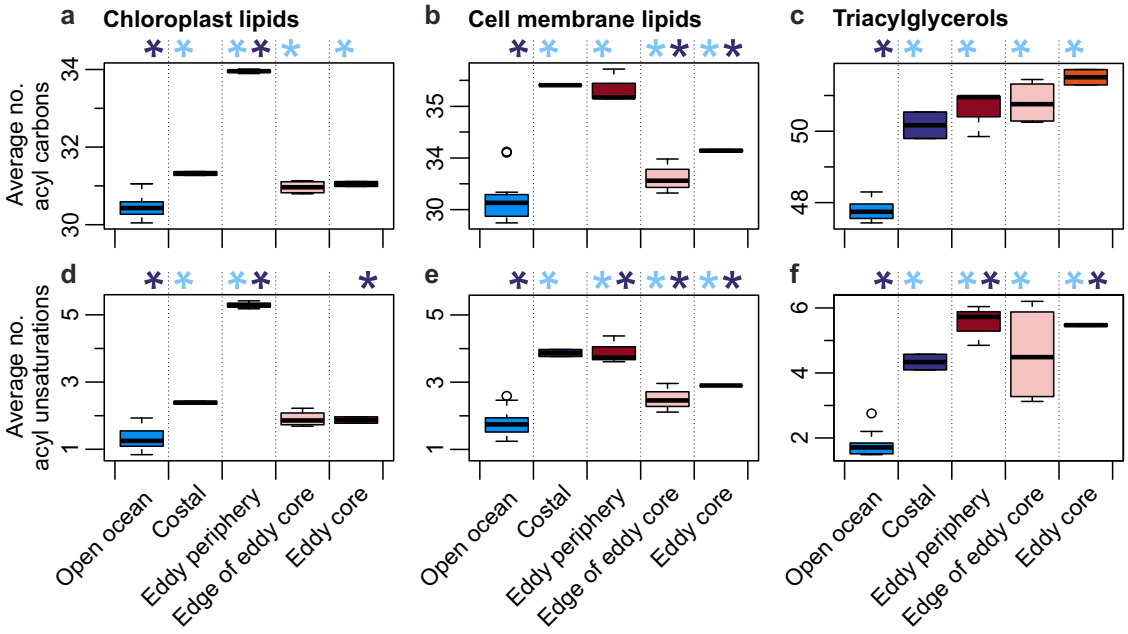

Fig. 5 | Acyl chain double bonds and carbon atoms in the identified clusters. Total average number of acyl carbon atoms and acyl unsaturations in chloroplast lipids (**a**, **d**), cell membrane lipids (**b**, **e**) and triacylglycerols (**c**, **f**) across the five clusters shown in Fig. 2. Boxes represent the interquartile ranges, the line within the box the median, and the whiskers extend to the minimum and maximum values within 1.5 times the interquartile range. Outliers are shown as circles. The chloroplast lipids include the glycolipids with diacylglycerol side chain (the galactolipids mono- and digalactosyldiacylglycerol and the sulfolipid sulfoquinovosyldiacylglycerol). The cell membrane lipids include all detected phospho- and betaine lipids. Asterisks indicate variables significantly different (one-way ANOVA, $p < 0.05$) from coastal (dark blue) and open-ocean (light blue) stations, respectively.

compared to all other stations with the higher values occurring in the periphery (Fig. 5; Supplementary Fig. 10). This indicates a higher content of long-chain polyunsaturated fatty acids (PUFA) in this region of the eddy. Indeed, the mass spectral analysis of the dominant long-chain, polyunsaturated compounds (MGDG 36:9 and MGDG 36:10) showed that the essential fatty acid eicosapentaenoic acid (20:5n3) is the dominant fatty acid in C_{36} and C_{38} diacylglycerols (Supplementary Fig. 11). The second fatty acid in MGDG 36:9 was a 16:4 fatty acid, which is used as a marker for diatoms[66], further supporting that larger eukaryotic phytoplankton were the dominant source of these lipids in the eddy periphery. The difference in fatty acid composition in the periphery is likely a result of the differences in phytoplankton community composition. While the chloroplast lipids were of predominantly cyanobacterial origin in the core of the eddy as well as the open ocean, larger eukaryotic phytoplankton were the dominant source of these lipids in the eddy periphery, which contain high abundances of PUFAs[32,54]. For cell membrane lipids and TAGs, differences only occurred between the eddy and the open ocean, but none was observed between the eddy-influenced stations and the coastal one (Fig. 5; Supplementary Fig. 12). This suggests invariant PUFA content in these lipid groups between the eukaryotic phytoplankton in the coast and the cyclonic eddy, but much lower PUFA content in open-ocean eukaryotic phytoplankton. Changes in temperature are well known to be one of the main drivers for changes in membrane unsaturation in a wide range of marine phytoplankton cultures[67–69]. Additionally, on the global scale, fatty acid unsaturation has recently been shown to be driven by temperature irrespective of the plankton community[28]. However, temperature variations were small in our local data set (Supplementary Fig. 2). Thus, our results indicate that shifts in phytoplankton group dominance due to mesoscale eddy activity can be the dominant driver for fatty acid unsaturation on local scales.

Drivers of surface ocean lipidome changes in and around a cyclonic eddy

Our results revealed that the cyclonic eddy formed in the EBUS off Mauritania carried a distinct lipidome signature indicative of enhanced abundance of eukaryotic phytoplankton, bacterial and archaeal biomass compared to the surrounding coastal and open-ocean stations. Since the eddy formed near the coast when upwelling still occurred, but it was sampled during the following relaxation season (see Material and Methods; Supplementary Fig. 3), the lipid composition could reflect the composition found near the coast at the time of eddy formation. Eddy trapping of coastal waters together with the supply of nutrients into the euphotic zone by shoaling the pycnocline likely sustains productivity of the coastal community during westward propagation. There was strong spatial variability in lipid distribution within the eddy in line with our previous observations of a spatial mosaic of microbial processes within this eddy[7]. This variability can be associated with eddy dynamics. Satellite measurements of upper-ocean chlorophyll revealed that horizontal advection of chlorophyll by the rotational velocity within the interior of eddies results in dipoles with extrema outside of the eddy cores, rather than monopoles of positive or negative chlorophyll anomalies trapped at the eddy cores[70]. In westward-propagating cyclones that rotate anticlockwise in the Northern Hemisphere, anomalously high and low chlorophyll concentrations typically occur in the southwest and northeast quadrants of the eddy, respectively, but upwelling of nutrient-rich water can still result in high chlorophyll concentrations in the core through enhanced phytoplankton production[10]. Nutrients are also transported laterally within eddies via advection and diffusion[71–73] affecting phytoplankton distributions on the submesoscale[74]. Thus, both vertical and lateral processes on the submesoscale affect the distribution of plankton in eddies leading to patchy phytoplankton distribution and activity[7,75,76] and are likely the driver for the observed variations in lipid composition within the eddy. Interestingly, the core of the eddy appears to consolidate important members of the microbial community involved in different processes of the carbon and nutrient cycles through the increased presence of not only photoautotrophic cyanobacteria and heterotrophic bacteria, but also chemoautotrophic ammonia oxidizing Nitrososphaerota in the surface mixed layer as indicated by specific lipid biomarkers for these microbial groups. Lipids provide information mainly about biomass, but not necessarily activity. However, a recent study of a cyclonic eddy in the subtropical Pacific

showed enhanced ammonia and nitrite oxidation rates in the euphotic zone indicating that mesoscale mechanisms can affect the distribution of marine nitrifiers[53]. Future studies combining lipidomics with 16S and 18S diversity data will shed further light on the relationship between changes in microbial community composition and lipid diversity in mesoscale eddies. Additionally, the study of other omics, such as metatranscriptomic surveys of lipid biosynthesis genes, will be useful for linking microbial community dynamics within eddies to lipid distributions.

Effects of lipid distributional changes for the nutritional quality of phytoplankton

The profound impact of the eddy on the microbial lipidome and with this its biochemical composition has further implications for the nutritional quality of the microbes and in particular the phytoplankton. The strong enrichment in TAG storage lipids together with the higher concentration of PUFA in the periphery of eddy suggest that eukaryotic phytoplankton in this region, which are mainly diatoms, are a food source of superior quality for zooplankton compared to non-cyclonic eddy influenced areas. Lipids provide the densest form of energy in the marine environment and contain more than twice the energy per gram compared to carbohydrates or proteins[32,77]. Additionally, PUFAs are essential fatty acids that are provided by the phytoplankton to higher trophic levels that cannot synthesize these molecules and must obtain them through their diet[32,54]. The enrichment of these nutritious lipids is thus a plausible driver of the observed changes in zooplankton feeding behavior and population dynamics in the periphery of cyclonic eddies[78–82] that ultimately contribute to fisheries resources. It has recently also been shown that human fishing activities are linked to mesoscale eddy activity with highest fishing activities occurring at the margins of cyclones[83], which we associate to the high nutritional quality of the phytoplankton. Variability in phytoplankton community composition has further been shown to result in strongly enhanced export of carbon at the periphery of eddies due to high diatom abundances[82]. Mesoscale eddies can thus efficiently transfer CO_2 from the atmosphere to deep waters via the biological carbon pump, but with horizontal variability depending on the position within the eddy. Although the sampling of eddies is difficult due to their transient nature, our lipidomics results support the view that considering spatial heterogeneity within these features will be important for more accurate predictions of the effects of eddies on oceanic carbon cycling[75].

Lateral export of lipid carbon from the Mauritanian upwelling area to the open ocean

During westward propagation, mesoscale eddies formed in EBUS can travel hundreds of kilometers into the subtropical gyres, where they may be involved in supporting the relatively high productivities – elevated biological productivity has been shown to be sustained across the extensive ocean subtropical gyres, but the underlying mechanisms have been under debate for decades[20–23]. Quantitatively important amounts of POC have been shown to be exported from the California coastal upwelling region to the gyres by mesoscale eddies with an eddy-induced enrichment of more than 20 Gg year^{-1} [17] potentially providing labile carbon for the open-ocean microbes and other organisms. Similarly, model simulations suggest lateral POC export from the Mauritanian upwelling system to the open ocean to be in the Gg to Tg C year^{-1} range[84]. Based on our quantitative lipid analysis from the cyclonic eddy, we estimated the amount of lipids carried in the surface mixed layer through the sustained productivity from the Mauritanian upwelling region to the subtropical gyre within cyclonic eddies using the modeling results from Schütte et al.[16] for average cyclonic eddy dimensions (radius of 51 km) and the yearly number of cyclonic eddies that live long enough to propagate into the open ocean (3.9 eddies year^{-1}). With our observed mixed-layer-integrated lipid concentration averaged for all eddy stations of 203.6 ± 39.3 mg m^{-2} (Supplementary Fig. 13), this adds up to 12.9 ± 2.5 Gg lipid year^{-1}, which translates to 9.7 ± 2.0 Gg lipid C year^{-1}. Considering that all major EBUS are hotspots for eddy generation[85,86], cyclonic eddies may play a quantitatively important role in the lateral export of labile carbon in the form of energy and nutrient-rich lipids to the open ocean. Indeed, using the number of long-lived cyclonic eddies generated in the four major EBUS based on 10-year records of satellite-altimetry data and Argo float profiles of temperature and salinity from Pegliasco et al.[85] (between 40 and 50 cyclonic eddies in each EBUS), 1.8 Tg lipid C year^{-1} globally may be transported within the mixed layer from coastal upwelling regions to the open ocean. The fate of the energy-rich and essential lipid-producing phytoplankton upon decay of the eddy remains unknown, but will be an important target for future studies as the different agents of mortality differ in their impact on the aquatic food web and carbon cycling. While phytoplankton lysis (autolysis and viral lysis) results in the production of DOM available for heterotrophic microbes, potentially contributing to the often observed net heterotrophy in the open ocean[21], zooplankton grazing mortality transfers the carbon to higher trophic levels and enhances export of sinking organic matter from the upper ocean to depth[87]. Additionally, biological activity and particulate organic matter characteristics have been shown to be affected by the intensity and the age of eddies[88,89], which will have consequences for the quality of organic matter delivered to the open ocean. For example, a recent study in the California Current System showed that both the physicochemical and diatom community structure within cyclonic eddies evolve during propagation offshore with a depletion of nutrients leading to lower biological activities over time[8]. Modeling results further suggest that the carbon content of coastal cyclonic eddies decreases while propagating westward[84]. Our estimate of surface ocean lipid transport by cyclonic eddies thus likely represents the upper limit as the eddy was still in its intensification stage[35]. Understanding changes in lipid abundance and composition in the same eddy over time including its vertical structure as well as variability between eddies formed during different seasons will help to constrain the effect of the supplied carbon for the indigenous open-ocean community and the carbon cycle. To this end, future studies that follow eddies during their westward propagation from formation at the coast until decay in the open ocean and concomitant comprehensive biogeochemical analysis will be essential, especially since eddy activity is projected to change significantly in the future[90].

Material and methods

Sample collection

Seawater samples for lipidomics were collected during RV Meteor cruise M156[91] in the Eastern Tropical North Atlantic off Mauritania (see Fig. 1) using standard Niskin-type bottles attached to a CTD rosette. After collection, the samples (1 L) were filtered using vacuum filtration (ca. −200 mm Hg) onto 47 mm diameter 0.2 µm hydrophilic Durapore filters (Millipore) and immediately flash-frozen and stored at −80 °C until processing. Samples were collected from eleven stations, of which six were located within the zonal eddy passage at 18°N between the Mauritanian Shelf and the Cape Verde Islands. One of these stations (E3) was just beyond the southwestern periphery of a cyclonic eddy, which was identified during the cruise based on satellite imagery (sea surface height) and ship-based Acoustic Doppler Current Profiler analysis. Four additional stations were located inside of the eddy-influenced waters with two of them (EDM4 and EDM5E) at the edge of the eddy core, one inside of the core (EDM4E) and one in the southwestern periphery (EDZ1). As a reference site, the Cape Blanc (CB) time series station (21°10.037'N, 20°54.983'W) was sampled. The exact location of the eddy center was validated and refined by Acoustic Doppler Current Profiler (ADCP) reconstructions and assuming an axis-symmetric vortex analysis (see Supplementary Methods). For details about the eddy identification the reader is also referred Devresse et al.[7]. We have further used an angular momentum eddy detection and tracking algorithm (AMEDA)[92] to estimate the age and origin of the eddy. This analysis revealed that the eddy formed near the coast, was 1.5 months old and still in the intensification stage during sampling[7] (see Supplementary Fig. 3a). While the upwelling season is typically from December to April[93], satellite-derived chlorophyll concentrations together with the reconstructed ADT

using AMEDA from the time of eddy formation in May indicates that coastal upwelling has still occurred at that time and that the sampling in July took place during the relaxation phase (see Supplementary Fig. 3b).

Lipid extraction and analysis

For lipidomics analysis, samples from the surface mixed layer only were selected (Supplementary Table 1) in this study. Lipids were ultrasonically extracted following a modified Bligh & Dyer protocol[94] using a monophasic mixture of methanol, dichloromethane, and 50 mM phosphate buffer at pH 7.4 (2:1:0.8, v:v:v). 1,2 dihenarachidoyl-sn-glycero-3-phosphocholine (Avanti Polar Lipids, Alabaster, AL, USA) was used as internal standard. The total lipid extracts (TLE) were dried under a stream of N_2 and stored at −20 °C until measurement.

Lipids were analyzed by injecting TLE aliquots dissolved in methanol:dichloromethane (9:1, v:v) on a Dionex Ultimate 3000 high performance liquid chromatography (HPLC) system connected to a Bruker maXis Ultra-High Resolution quadrupole time-of-flight tandem mass spectrometer (MS) equipped with an ESI ion source operating in positive mode (Bruker Daltonik, Bremen, Germany). The MS was set to a resolving power of 27,000 at *m/z* 1222 and every analysis was mass-calibrated by loop injections of a calibration standard and correction by lock mass, leading to a mass accuracy of better than 1–3 ppm[95].

Analyte separation was achieved using reversed phase HPLC on an Acquity UPLC BEH C_{18} column (1.7 µm, 2.1 × 150 mm, Waters, Eschborn, Germany) maintained at 65 °C as described by Wörmer et al.[96]. Analytes were eluted at a flow rate of 0.4 mL min^{-1} using linear gradients of methanol:water (85:15, v:v, eluent A) to methanol:isopropanol (50:50, v:v, eluent B) both with 0.04% formic acid and 0.1% NH_3. The initial condition was 100% A held for 2 min, followed by a gradient to 15% B in 0.1 min and a gradient to 85% B in 18 min. The column was then washed with 100% B for 8 min.

The samples were additionally analyzed on the same system under different chromatographic conditions using normal phase HPLC on an Acquity UPLC BEH Amide column (1.7 µm, 2.1 × 150 mm; Waters Corporation, Eschborn, Germany) maintained at 40 °C as described by Wörmer et al.[96]. Aliquots of the TLE were dissolved in dichloromethane:methanol (9:1, v:v) and analytes were eluted at a flow rate of 0.5 ml min^{-1} with 99 % eluent A (acetonitrile:dichloromethane, 75:25, with 0.01 % formic acid and NH_3, v:v:v:v) and 1% eluent B (methanol:water, 50:50, with 0.4 % formic acid and NH_3) for 2.5 min, increasing B to 5% at 4 min, to 20% B at 22.5 min and 40% B at 26.5 min. The column was then flushed with 40% B for 1 min.

Lipids were identified by retention time as well as accurate molecular mass and isotope pattern match of proposed sum formulas in full scan mode and MS^2 fragment spectra[39,94,97,98] (see Supplementary Figs. 5 and 6 for representative MS^2 spectra of each compound group). The normal phase HPLC-MS analysis was used for bacterial and eukaryotic intact polar lipid detection, while reversed phase HPLC-MS analysis was used for archaeal lipids, pigments, respiratory quinones and triacylglycerols (TAGs). Integration of peaks was performed on extracted ion chromatograms of ±10 mDa width and included the $[M + H]^+$, $[M + NH_4]^+$ and $[M+Na]^+$ ions using Data Analysis™ and Quant Analysis™ software (Bruker Daltonik, Bremen, Germany). Where applicable, doubly charged ions were included in the integration. Lipid quantification was achieved by comparison of parent ion responses relative to known amounts of the internal standard. Lipid concentrations were corrected for response factors of commercially available standards in external standard curves. For phosphoethanolamine (PE), phosphocholine (PC), and phosphatidylglycerol (PG), 1,2-dipalmitoyl-sn-glycero-3-PE, -PC, and -PG, standards were used, respectively (Avanti Polar Lipids, Alabaster, AL, USA). Monogalactosyldiacylglycerol (MGDG), digalactosyldiacylglycerol (DGDG), sulfoquinovosyldiacylglycerol (SQDG) standards from Avanti Polar Lipids were used to correct MGDG, DGDG and SQDG, respectively. For the betaine lipids Diacylglyceryl-carboxyhydroxymethylcholine, Diacylglycerylhydroxy-methyltrimethylalanine and Diacylglyceryltrimethylhomoserine, a Diacylglyceryltrimethylhomoserine standard also from Avanti Polar Lipids was used. Quinone concentrations were corrected for the relative response of menaquinone (MK; $MK_{4:4}$ for MKs and vitamin K_1) and ubiquinone (UQ; $UQ_{10:10}$ for UQs, and plastoquinones) standards (Sigma-Aldrich, St. Louis, MO, USA). For chlorophylls and their degradation products, a chlorophyll *a* standard and for carotenoids an astaxanthin standard also from Sigma-Aldrich was used. TAGs were quantified using a series of individual standards from Nu-Check-Prep, (Elysian, MN, USA). TAG response factors were based on the equivalent carbon number of each TAG after Holčapek et al.[99]. Purified archaeal lipid standards were obtained from extracts of *Archaeoglobus fulgidus* as described by Elling et al.[100]. The concentrations of monohexose glycerol dibiphytanyl glycerol tetraethers (GDGTs) were corrected for the response of a purified acyclic monohexose GDGT standard. The concentration of GDGT core lipids and glycerol dibiphytanol diethers were corrected for the response factors of purified acyclic GDGT as described previously[100], while the concentration of archaeol was corrected for the response factor of the respective purified standard. The lower limit of detection for lipids was <1 pg on column. Isotopically labeled standards are not needed for samples from the surface ocean[39]. For normal phase HPLC-MS analysis, peak areas were additionally corrected for isotopic overlying effects from co-eluting molecular species containing an additional double bond by subtracting the intensity contributed from the natural abundance of isotopologues (e.g., the $2x^{13}C$ containing isotopologues). For example, PC 30:1 containing $2x^{13}C$ atoms has a molecular mass of 706.5288 and PC 30:0 with only ^{12}C atoms as a mass of 706.5381, which cannot be distinguished with the used methods. The natural abundance of $2x^{13}C$ PC 30:1 is 10.5% compared to an only ^{12}C-containing PC 30:1. Thus, 10.5% of the peak area of PC 30:1 was subtracted from the peak area of PC 30:0. Higher isotopologues were neglected due to their low natural abundance (<1%).

Weighted mean calculations

A weighted arithmetic mean of lipid species concentrations was used to describe the average number of acyl carbon atoms and the average number of unsaturations in the acyl-containing lipid groups. They were calculated as follows:

$$Average\ no.\ of\ acyl\ carbon\ atoms = \left(\sum [C\,x\,\%lipid]\right)/100 \quad (1)$$

where *C* is the total number of acyl chain carbons and %lipid the percent abundance of all lipids with *C* amount of carbon.

$$Average\ no.\ of\ acyl\ unsaturations = \left(\sum [U\,x\,\%lipid]\right)/100 \quad (2)$$

where *U* is the total number of acyl chain unsaturations and %lipid the percent abundance of all lipids with *U* amount of unsaturations.

Particulate organic carbon analysis

For analyses of particulate organic carbon, water samples (0.5–1 L) were filtered onto pre–combusted (450 °C for 5 h) Whatman GF/F filters (25 mm, 0.7 µm) under low pressure (<200 mbar). Filters were stored frozen at −20 °C until analysis. Prior to analysis, filters were acid–fumed (37% HCl for 24 h) in order to remove inorganic carbon and dried at 40 °C for 24 h. Subsequently, filters were wrapped in tin cups (8 × 8 × 15 mm) and analyzed according to Sharp[101] using a EuroEA Elemental Analyzer (HEKAtech, Wegberg, Germany). Blank filters were used to correct for contaminations.

Hierarchical clustering analysis

The hierarchical clustering analysis was carried out using R version 4.3.0 on lipid concentrations (ng L^{-1}) converted into log-space to account for the large value range. First, the Euclidean distance matrix was calculated using the dist function. Then, the hierarchical clustering analysis was performed using the hclust function with default parameters and the average linking

method. The functions dist and hclust are built-in functions in R. Clustered heatmaps were generated using the R package pheatmap[102].

Data availability

All data are publicly available in the Pangaea database: Lipidomics data, https://doi.org/10.1594/PANGAEA.974978; CTD data including temperature and salinity, https://doi.org/10.1594/PANGAEA.943431; particulate organic carbon data, https://doi.org/10.1594/PANGAEA.964733; dissolved ammonium data, https://doi.org/10.1594/PANGAEA.950358; ADCP data, https://doi.org/10.1594/PANGAEA.943408.

Received: 26 January 2024; Accepted: 20 February 2025;
Published online: 04 March 2025

References

1. Field, C. B., Behrenfeld, M. J., Randerson, J. T. & Falkowski, P. Primary production of the biosphere: Integrating terrestrial and oceanic components. *Science* **281**, 237–240 (1998).
2. Falkowski, P. Ocean science: The power of plankton. *Nature* **483**, S17–S20 (2012).
3. Sigman, D. M. & Hain, M. P. The biological productivity of the ocean. *Nat. Educ. Knowl.* **3**, 21 (2012).
4. Gaube, P., McGillicuddy, D. J. Jr. & Moulin, A. J. Mesoscale Eddies modulate mixed layer depth globally. *Geophys. Res. Lett.* **46**, 1505–1512 (2019).
5. Bibby, T. S., Gorbunov, M. Y., Wyman, K. W. & Falkowski, P. G. Photosynthetic community responses to upwelling in mesoscale eddies in the subtropical North Atlantic and Pacific Oceans. *Deep Sea Res. Part II Top. Stud. Oceanogr.* **55**, 1310–1320 (2008).
6. Baltar, F., Arístegui, J., Gasol, J. M., Lekunberri, I. & Herndl, G. J. Mesoscale eddies: hotspots of prokaryotic activity and differential community structure in the ocean. *ISME J.* **4**, 975–988 (2010).
7. Devresse, Q., Becker, K. W., Bendinger, A., Hahn, J. & Engel, A. Eddy-enhanced primary production sustains heterotrophic microbial activities in the Eastern Tropical North Atlantic. *Biogeosciences* **19**, 5199–5219 (2022).
8. Abdala, Z. M. et al. Examining ecological succession of diatoms in California Current System cyclonic mesoscale eddies. *Limnol. Oceanogr.* **67**, 2586–2602 (2022).
9. McGillicuddy, D. J. Jr. & Robinson, A. R. Eddy-induced nutrient supply and new production in the Sargasso Sea. *Deep Sea Res. Part I Oceanogr. Res. Pap.* **44**, 1427–1450 (1997).
10. McGillicuddy, D. J. Jr. Mechanisms of physical-biological-biogeochemical interaction at the oceanic mesoscale. *Ann. Rev. Mar. Sci.* **8**, 125–159 (2016).
11. Mahadevan, A. & Archer, D. Modeling the impact of fronts and mesoscale circulation on the nutrient supply and biogeochemistry of the upper ocean. *J. Geophys. Res. Ocean.* **105**, 1209–1225 (2000).
12. Levy, M., Memery, L. & Madec, G. The onset of a bloom after deep winter convection in the northwestern Mediterranean sea: mesoscale process study with a primitive equation model. *J. Mar. Syst.* **16**, 7–21 (1998).
13. Belkin, N. et al. Influence of cyclonic and anti-cyclonic eddies on plankton biomass, activity and diversity in the southeastern Mediterranean Sea. *Ocean Sci. Discuss.* **18**, 1–56 (2022).
14. Zhang, M. et al. Hotspot of organic carbon export driven by mesoscale eddies in the slope region of the northern south China sea. *Front. Mar. Sci.* **7**, 444 (2020).
15. Bent, S. M. et al. Lipid biochemical diversity and dynamics reveal phytoplankton nutrient-stress responses and carbon export mechanisms in mesoscale eddies in the North Pacific Subtropical Gyre. *Front. Mar. Sci.* **11**, 1427524 (2024).
16. Schütte, F. et al. Characterization of "dead-zone" eddies in the eastern tropical North Atlantic. *Biogeosciences* **13**, 5865–5881 (2016).
17. Amos, C. M., Castelao, R. M. & Medeiros, P. M. Offshore transport of particulate organic carbon in the California Current System by mesoscale eddies. *Nat. Commun.* **10**, 4940 (2019).
18. Combes, V. et al. Cross-shore transport variability in the California Current: Ekman upwelling vs. eddy dynamics. *Prog. Oceanogr.* **109**, 78–89 (2013).
19. Nagai, T. et al. Dominant role of eddies and filaments in the offshore transport of carbon and nutrients in the California Current System. *J. Geophys. Res. Ocean.* **120**, 5318–5341 (2015).
20. Lovecchio, E., Gruber, N., Münnich, M. & Frenger, I. On the processes sustaining biological production in the offshore propagating eddies of the northern canary upwelling system. *J. Geophys. Res. Ocean.* **127**, e2021JC017691 (2022).
21. Duarte, C. M., Regaudie-de-Gioux, A., Arrieta, J. M., Delgado-Huertas, A. & Agustí, S. The oligotrophic ocean is heterotrophic. *Ann. Rev. Mar. Sci.* **5**, 551–569 (2013).
22. Williams, P. JleB., Quay, P. D., Westberry, T. K. & Behrenfeld, M. J. The oligotrophic ocean is autotrophic. *Ann. Rev. Mar. Sci.* **5**, 535–549 (2013).
23. Gupta, M. et al. A nutrient relay sustains subtropical ocean productivity. *Proc. Natl. Acad. Sci. USA* **119**, e2206504119 (2022).
24. Kharbush, J. J. et al. Particulate organic carbon deconstructed: molecular and chemical composition of particulate organic carbon in the ocean. *Front. Mar. Sci.* **7**, 518 (2020).
25. Wakeham, S. G., Hedges, J. I., Lee, C., Peterson, M. L. & Hernes, P. J. Compositions and transport of lipid biomarkers through the water column and surficial sediments of the equatorial Pacific Ocean. *Deep Sea Res. Part II Top. Stud. Oceanogr.* **44**, 2131–2162 (1997).
26. Van Mooy, B. A. S. et al. Phytoplankton in the ocean use non-phosphorus lipids in response to phosphorus scarcity. *Nature* **458**, 69–72 (2009).
27. Wörmer, L., Lipp, J. S. & Hinrichs, K.-U. Comprehensive analysis of microbial lipids in environmental samples through HPLC-MS protocols. In *Hydrocarb. lipid Microbiol. Protoc. Pet. Hydrocarb. lipid Anal*. (eds McGenity, T. J., Timmis, K. N. & Nogales, B.) 289–317 (Springer, Berlin, Heidelberg, 2015).
28. Holm, H. C. et al. Global ocean lipidomes show a universal relationship between temperature and lipid unsaturation. *Science* **376**, 1487–1491 (2022).
29. Schubotz, F., Wakeham, S. G., Lipp, J. S., Fredricks, H. F. & Hinrichs, K.-U. Detection of microbial biomass by intact polar membrane lipid analysis in the water column and surface sediments of the Black Sea. *Environ. Microbiol.* **11**, 2720–2734 (2009).
30. Van Mooy, B. A. S. & Fredricks, H. F. Bacterial and eukaryotic intact polar lipids in the eastern subtropical South Pacific: Water-column distribution, planktonic sources, and fatty acid composition. *Geochim. Cosmochim. Acta* **74**, 6499–6516 (2010).
31. Schouten, S. et al. Intact polar and core glycerol dibiphytanyl glycerol tetraether lipids in the Arabian Sea oxygen minimum zone: I. Selective preservation and degradation in the water column and consequences for the TEX86. *Geochim. Cosmochim. Acta* **98**, 228–243 (2012).
32. Parrish, C. C. Lipids in Marine Ecosystems. *ISRN Oceanogr.* **2013**, 1–16 (2013).
33. Faghmous, J. H. et al. A daily global mesoscale ocean eddy dataset from satellite altimetry. *Sci. Data* **2**, 1–16 (2015).
34. Popendorf, K. J. et al. Gradients in intact polar diacylglycerolipids across the Mediterranean Sea are related to phosphate availability. *Biogeosciences* **8**, 3733–3745 (2011).
35. Devresse, Q., Becker, K. W. & Engel, A. Distribution of polysaccharidic and proteinaceous gel− like particles in three cyclonic eddies in the Eastern Tropical North Atlantic. *Front. Mar. Sci.* **11**, 1357646 (2024).
36. Devresse, Q., Becker, K. W., Dilmahamod, A. F., Ortega-Retuerta, E. & Engel, A. Dissolved organic matter fluorescence as a tracer of

upwelling and microbial activities in Two Cyclonic Eddies in the Eastern Tropical North Atlantic. *J. Geophys. Res. Ocean.* **128**, e2023JC019821 (2023).
37. Beech, N. et al. Long-term evolution of ocean eddy activity in a warming world. *Nat. Clim. Chang.* **12**, 910–917 (2022).
38. Hu, Q. et al. Microalgal triacylglycerols as feedstocks for biofuel production: perspectives and advances. *Plant J.* **54**, 621–639 (2008).
39. Becker, K. W. et al. Daily changes in phytoplankton lipidomes reveal mechanisms of energy storage in the open ocean. *Nat. Commun.* **9**, 5179 (2018).
40. Nowicka, B. & Kruk, J. Occurrence, biosynthesis and function of isoprenoid quinones. *Biochim. Biophys. Acta* **1797**, 1587–1605 (2010).
41. Bachmann, J. et al. Environmental drivers of free-living vs. particle-attached bacterial community composition in the Mauritania upwelling system. *Front. Microbiol.* **9**, 2836 (2018).
42. Kondo, M. et al. slr2103, a homolog of type-2 diacylglycerol acyltransferase genes, for plastoquinone-related neutral lipid synthesis and NaCl-stress acclimatization in a cyanobacterium, Synechocystis sp. PCC 6803. *Front. Plant Sci.* **14**, 1181180 (2023).
43. Becker, K. W. et al. Isoprenoid quinones resolve the stratification of microbial redox processes in a biogeochemical continuum from the photic zone to deep anoxic sediments of the Black Sea. *Appl. Environ. Microbiol.* **84**, e02736-17 (2018).
44. Nitschke, W., Kramer, D. M., Riedel, A. & Liebl, U. From naphtho- to benzoquinones -(r)evolutionary reorganizations of electron transfer chains. In *Photosynthesis: From Light to Biosphere* (ed. Mathis, P.) 945–950 (Kluwer Academic, 1995).
45. Collins, M. D. & Jones, D. Distribution of isoprenoid quinone structural types in bacteria and their taxonomic implications. *Microbiol. Rev.* **45**, 316–354 (1981).
46. Pitcher, A. et al. Niche segregation of ammonia-oxidizing archaea and anammox bacteria in the Arabian Sea oxygen minimum zone. *ISME J.* **5**, 1896–1904 (2011).
47. Schouten, S., Middelburg, J. J., Hopmans, E. C. & Sinninghe Damsté, J. S. Fossilization and degradation of intact polar lipids in deep subsurface sediments: A theoretical approach. *Geochim. Cosmochim. Acta* **74**, 3806–3814 (2010).
48. Logemann, J. et al. A laboratory experiment of intact polar lipid degradation in sandy sediments. *Biogeosciences* **8**, 2547–2560 (2011).
49. Xie, S., Lipp, J. S., Wegener, G., Ferdelman, T. G. & Hinrichs, K. Turnover of microbial lipids in the deep biosphere and growth of benthic archaeal populations. *Proc. Natl. Acad. Sci. USA* **110**, 6010–6014 (2013).
50. Hurley, S. J., Lipp, J. S., Close, H. G., Hinrichs, K.-U. & Pearson, A. Distribution and export of isoprenoid tetraether lipids in suspended particulate matter from the water column of the Western Atlantic Ocean. *Org. Geochem.* **116**, 90–102 (2018).
51. Li, F. et al. Planktonic archaeal ether lipid origins in surface waters of the North Pacific subtropical gyre. *Front. Microbiol.* **12**, 610675 (2021).
52. Könneke, M. et al. Isolation of an autotrophic ammonia-oxidizing marine archaeon. *Nature* **437**, 543–546 (2005).
53. Liu, L. et al. Reduced nitrite accumulation at the primary nitrite maximum in the cyclonic eddies in the western North Pacific subtropical gyre. *Sci. Adv.* **9**, eade2078 (2023).
54. Jónasdóttir, S. H. Fatty acid profiles and production in Marine Phytoplankton. *Mar. Drugs* **17**, 151 (2019).
55. Lochte, K. & Pfannkuche, O. Cyclonic cold-core eddy in the eastern North Atlantic. II. Nutrients, phytoplankton and bacterioplankton. *Mar. Ecol. Prog. Ser.* **39**, 153–164 (1987).
56. McGillicuddy, D. J. et al. Eddy/Wind interactions stimulate extraordinary mid-ocean plankton blooms. *Science* **316**, 1021–1026 (2007).
57. Williams, R. & Claustre, H. Photosynthetic pigments as biomarkers of phytoplankton populations and processes involved in the transformation of particulate organic matter at the Biotrans site (47°N, 20°W). *Deep Sea Res. Part A. Oceanogr. Res. Pap.* **38**, 347–355 (1991).
58. Goericke, R. & Repeta, D. J. The pigments of Prochlorococcus marinus: The presence of divinylchlorophyll a and b in a marine procaryote. *Limnol. Oceanogr.* **37**, 425–433 (1992).
59. Partensky, F., Hess, W. R. & Vaulot, D. Prochlorococcus, a marine photosynthetic prokaryote of global significance. *Microbiol. Mol. Biol. Rev.* **63**, 106–127 (1999).
60. Bidigare, R. R. et al. Observations of a Synechococcus-dominated cyclonic eddy in open-oceanic waters of the Arabian Sea. In *Ocean Optics XIII* **2963**, 260–265 (SPIE, 1997).
61. Stevens, H., Brinkhoff, T., Rink, B., Vollmers, J. & Simon, M. Diversity and abundance of Gram positive bacteria in a tidal flat ecosystem. *Environ. Microbiol.* **9**, 1810–1822 (2007).
62. Elling, F. J. et al. Chemotaxonomic characterisation of the thaumarchaeal lipidome. *Environ. Microbiol.* **19**, 2681–2700 (2017).
63. Zapata, M. et al. Photosynthetic pigments in 37 species (65 strains) of Haptophyta: implications for oceanography and chemotaxonomy. *Mar. Ecol. Prog. Ser.* **270**, 83–102 (2004).
64. Menschel, E., González, H. E. & Giesecke, R. Coastal-oceanic distribution gradient of coccolithophores and their role in the carbonate flux of the upwelling system off Concepción, Chile (36°S). *J. Plankton Res.* **38**, 798–817 (2016).
65. Jónasdóttir, S. H., Visser, A. W., Richardson, K. & Heath, M. R. Seasonal copepod lipid pump promotes carbon sequestration in the deep North Atlantic. *Proc. Natl. Acad. Sci. USA* **112**, 12122–12126 (2015).
66. Dunstan, G. A., Volkman, J. K., Barrett, S. M., Leroi, J.-M. & Jeffrey, S. W. Essential polyunsaturated fatty acids from 14 species of diatom (Bacillariophyceae). *Phytochemistry* **35**, 155–161 (1993).
67. Thompson, P. A., Guo, M., Harrison, P. J. & Whyte, J. N. C. Effects of variation in temperature. II. On the fatty acid composition of eight species of marine phytoplankton 1. *J. Phycol.* **28**, 488–497 (1992).
68. Jiang, H. & Gao, K. Effects of lowering temperature during culture on the production of polyunsaturated fatty acids in the marine diatom Phaeodactylum tricornutum (bacillariophyceae). *J. Phycol.* **40**, 651–654 (2004).
69. Pittera, J. et al. Thermoacclimation and genome adaptation of the membrane lipidome in marine Synechococcus. *Environ. Microbiol.* **20**, 612–631 (2018).
70. Chelton, D. B., Gaube, P., Schlax, M. G., Early, J. J. & Samelson, R. M. The influence of nonlinear mesoscale eddies on Near-Surface Oceanic Chlorophyll. *Science* **334**, 328–332 (2011).
71. Lee, M.-M. & Williams, R. G. The role of eddies in the isopycnic transfer of nutrients and their impact on biological production. *J. Mar. Res.* **58**, 895–917 (2000).
72. Williams, R. G. & Follows, M. J. Physical transport of nutrients and the maintenance of biological production. In *Ocean Biogeochemistry: The Role of the Ocean Carbon Cycle in Global Change* 19–51 (Springer, 2003).
73. Resplandy, L. et al. Contribution of mesoscale processes to nutrient budgets in the Arabian Sea. *J. Geophys. Res. Ocean*. **116**, C1107 (2011).
74. Lévy, M., Ferrari, R., Franks, P. J. S., Martin, A. P. & Rivière, P. Bringing physics to life at the submesoscale. *Geophys. Res. Lett*. **39**, L14602 (2012).
75. Mahadevan, A. The impact of submesoscale physics on primary productivity of plankton. *Ann. Rev. Mar. Sci.* **8**, 161–184 (2016).
76. Lévy, M., Franks, P. J. S. & Smith, K. S. The role of submesoscale currents in structuring marine ecosystems. *Nat. Commun.* **9**, 4758 (2018).

77. Berg, J. M., Tymoczko, J. L. & Stryer, L. in *Biochemistry* 5th edn, 1050 (Freeman, W. H., 2002).
78. Beckmann, W., Auras, A. & Hemleben, C. Cyclonic cold-core eddy in the eastern North Atlantic. III. Zooplankton. *Mar. Ecol. Prog. Ser.* **39**, 165–173 (1987).
79. Goldthwait, S. A. & Steinberg, D. K. Elevated biomass of mesozooplankton and enhanced fecal pellet flux in cyclonic and mode-water eddies in the Sargasso Sea. *Deep Sea Res. Part II Top. Stud. Oceanogr.* **55**, 1360–1377 (2008).
80. Eden, B. R., Steinberg, D. K., Goldthwait, S. A. & McGillicuddy, D. J. Zooplankton community structure in a cyclonic and mode-water eddy in the Sargasso Sea. *Deep Sea Res. Part I Oceanogr. Res. Pap.* **56**, 1757–1776 (2009).
81. Schmid, M. S. et al. Prey and predator overlap at the edge of a mesoscale eddy: fine-scale, in-situ distributions to inform our understanding of oceanographic processes. *Sci. Rep.* **10**, 921 (2020).
82. Shih, Y.-Y. et al. Enhanced particulate organic carbon export at eddy edges in the Oligotrophic Western North Pacific Ocean. *PLoS One* **10**, e0131538 (2015).
83. Xing, Q., Yu, H., Wang, H., Ito, S. & Chai, F. Mesoscale eddies modulate the dynamics of human fishing activities in the global midlatitude ocean. Fish Fisheries **24**, 527–543 (2023).
84. Lovecchio, E., Gruber, N. & Münnich, M. Mesoscale contribution to the long-range offshore transport of organic carbon from the Canary Upwelling System to the open North Atlantic. *Biogeosciences* **15**, 5061–5091 (2018).
85. Pegliasco, C., Chaigneau, A. & Morrow, R. Main eddy vertical structures observed in the four major Eastern Boundary Upwelling Systems. *J. Geophys. Res. Ocean.* **120**, 6008–6033 (2015).
86. McWilliams, J. C. Submesoscale currents in the ocean. *Proc. R. Soc. A Math. Phys. Eng. Sci.* **472**, 20160117 (2016).
87. Steinberg, D. K. & Landry, M. R. Zooplankton and the ocean carbon cycle. *Ann. Rev. Mar. Sci.* **9**, 413–444 (2017).
88. Harke, M. J. et al. Microbial community transcriptional patterns vary in response to mesoscale forcing in the North Pacific Subtropical Gyre. *Environ. Microbiol.* **23**, 4807–4822 (2021).
89. Soares, M. A. et al. Variation of particulate organic matter characteristics in the upper water column of eddy-influenced waters at the subtropical front of the Indian sector of the Southern Ocean. *J. Sea Res.* **174**, 102074 (2021).
90. Martínez-Moreno, J. et al. Global changes in oceanic mesoscale currents over the satellite altimetry record. *Nat. Clim. Chang.* **11**, 397–403 (2021).
91. Sommer, S. et al. Role of Eddies in the Carbon Pump of Eastern Boundary Upwelling Systems, REEBUS, Cruise No. M156, 03.07.–01.08. 2019 Mindelo (Cap Verde)–Mindelo. (2020).
92. Le Vu, B., Stegner, A. & Arsouze, T. Angular momentum eddy detection and tracking algorithm (AMEDA) and its application to coastal eddy formation. *J. Atmos. Ocean. Technol.* **35**, 739–762 (2018).
93. Klenz, T., Dengler, M. & Brandt, P. Seasonal variability of the mauritania current and hydrography at 18°N. *J. Geophys. Res. Ocean.* **123**, 8122–8137 (2018).
94. Popendorf, K. J., Fredricks, H. F. & Van Mooy, B. A. S. Molecular ion-independent quantification of polar glycerolipid classes in marine plankton using triple quadrupole MS. *Lipids* **48**, 185–195 (2013).
95. Becker, K. W., Lipp, J. S., Zhu, C., Liu, X.-L. & Hinrichs, K.-U. An improved method for the analysis of archaeal and bacterial ether core lipids. *Org. Geochem.* **61**, 34–44 (2013).
96. Wörmer, L., Lipp, J. S., Schröder, J. M. & Hinrichs, K.-U. Application of two new LC–ESI–MS methods for improved detection of intact polar lipids (IPLs) in environmental samples. *Org. Geochem.* **59**, 10–21 (2013).
97. Yoshinaga, M. Y. et al. Systematic fragmentation patterns of archaeal intact polar lipids by high-performance liquid chromatography/electrospray ionization ion-trap mass spectrometry. *Rapid Commun. Mass Spectrom.* **25**, 3563–3574 (2011).
98. Becker, K. W. et al. Combined pigment and metatranscriptomic analysis reveals highly synchronized diel patterns of phenotypic light response across domains in the open oligotrophic ocean. *ISME J.* **15**, 520–533 (2021).
99. Holčapek, M., Lísa, M., Jandera, P. & Kabátová, N. Quantitation of triacylglycerols in plant oils using HPLC with APCI-MS, evaporative light-scattering, and UV detection. *J. Sep. Sci.* **28**, 1315–1333 (2005).
100. Elling, F. J. et al. Effects of growth phase on the membrane lipid composition of the thaumarchaeon Nitrosopumilus maritimus and their implications for archaeal lipid distributions in the marine environment. *Geochim. Cosmochim. Acta* **141**, 579–597 (2014).
101. Sharp, J. H. Improved analysis for "particulate" organic carbon and nitrogen from seawater 1. *Limnol. Oceanogr.* **19**, 984–989 (1974).
102. Kolde, R. & Kolde, M. R. Package 'pheatmap'. *R Packag.* **1**, 790 (2015).
103. Schlitzer, R. Ocean data view. https://odv.awi.de/ (2022).
104. Elling, F. J. et al. Respiratory quinones in Archaea: phylogenetic distribution and application as biomarkers in the marine environment. *Environ. Microbiol.* **18**, 692–707 (2016).

Acknowledgements

We gratefully acknowledge valuable data discussions with Felix J. Elling, Marcus Dengler and Benjamin Pontiller. Tania Klüver and Jon Roa are thanked for their help with onboard sampling and Min Song for supporting the analysis of lipid standards. We thank Ahmad Fehmi Dilmahamod for help with the eddy characterization. We are grateful to the crew and the scientific shipboard party of the R/V Meteor cruise M156 (Chief scientist: Stefan Sommer). We further thank five anonymous reviewers for their constructive feedback. Funding was provided by the German Federal Ministry of Education and Research (grant no. 03F0815A).

Author contributions

K.W.B. and A.E. conceived and designed the research; A.E. acquired funding; K.-U.H. provided analytical infrastructure and protocols; K.W.B. and Q.D. performed onboard sampling; X.P.M. and K.W.B. measured lipidomics samples; K.W.B. conducted the research, analyzed the lipidomics data and wrote the original draft of the manuscript; all authors reviewed and commented on the final draft.

Funding

Open Access funding enabled and organized by Projekt DEAL.

Competing interests

The authors declare no competing interests.

Additional information

Supplementary information The online version contains supplementary material available at https://doi.org/10.1038/s43247-025-02152-0.

Correspondence and requests for materials should be addressed to Kevin W. Becker.

Peer review information *Communications Earth & Environment* thanks Vincenzo Alessandro Laudicella and the other, anonymous, reviewer(s) for their contribution to the peer review of this work. Primary Handling Editors: Annie Bourbonnais and Alireza Bahadori. A peer review file is available.